Journal of Nuclear Medicine, published on May 26, 2022 as doi:10.2967/jnumed.122.264071

Effective Treatment of Human Breast Carcinoma Xenografts with Single-Dose ^{211}At-Labeled Anti-HER2 Single Domain Antibody Fragment

Yutian Feng, Rebecca Meshaw, Xiao-Guang Zhao, Stephen Jannetti, Ganesan Vaidyanathan and Michael R. Zalutsky

Department of Radiology, Duke University Medical Center, Durham, North Carolina

Contact information for first author:

Yutian Feng, e-mail: yutian.feng@duke.edu, Tel: (919) 684-7121

Contact information for correspondence:

Michael R. Zalutsky, e-mail: zalut001@mc.duke.edu, Tel: (919) 684-7708

ORCHID:0000-0002-5456-0324

Word count: 5757

Financial support: NIH Grant CA42324 and Cereius, Inc.

Running Title: ^{211}At-labeled anti-HER2 sdAb TAT

ABSTRACT

Single-domain antibody fragments (sdAbs) are attractive for targeted α-particle therapy, particularly with ^{211}At, because of their rapid accumulation in tumor and clearance from normal tissues. Here, we evaluate the therapeutic potential of this strategy with 5F7 and VHH_1028 - two sdAbs that bind with high affinity to Domain IV of human epidermal growth factor receptor type 2 (HER2). **Methods:** The HER2-specific sdAbs and HER2-irrelevant VHH_2001 were labeled using *N*-succinimidyl-3-^{211}At-astato-5-guanidinomethyl benzoate (*iso*-^{211}At-SAGMB). The cytotoxicity of *iso*-^{211}At-SAGMB-5F7 and *iso*-^{211}At-SAGMB-VHH_2001 were compared on HER2-expressing BT474 breast carcinoma cells. Three experiments in mice with subcutaneous BT474 xenografts were performed to evaluate the therapeutic effectiveness of single doses of 1) *iso*-^{211}At-SAGMB-5F7 (0.7-3.0 MBq), 2) *iso*-^{211}At-SAGMB-VHH_1028 (1.0-3.0 MBq), and 3) *iso*-^{211}At-SAGMB-VHH_1028 and *iso*-^{211}At-SAGMB-VHH_2001 (~1.0 MBq). **Results:** Clonogenic survival of BT474 cells was reduced after exposure to *iso*-^{211}At-SAGMB-5F7 (D_0=1.313 kBq/mL) while *iso*-^{211}At-SAGMB-VHH_2001 was ineffective. Dose-dependent tumor growth inhibition was observed with ^{211}At-labeled HER2-specific 5F7 and VHH_1028 but not with HER2-irrelevant VHH_2001. At the 3.0 MBq dose, complete tumor regression was seen in 3 of 4 mice treated with *iso*-^{211}At-SAGMB-5F7 and 8 of 11 mice treated with *iso*-^{211}At-SAGMB-VHH_1028; prolongation in median survival was 495% and 414%, respectively. **Conclusion:** Combining rapidly internalizing, high-affinity HER2-targeted sdAbs with the *iso*-^{211}At-SAGMB residualizing prosthetic agent is a promising strategy for targeted α-particle therapy of HER2-expressing cancers.

Key words: Single-domain antibody fragment, α-emitter, radiopharmaceutical therapy, astatine-211, HER2, nanobody

INTRODUCTION

The human epidermal growth factor receptor type 2 (HER2) is overexpressed on breast, ovarian and gastric cancers (*1*) and frequently is associated with metastatic progression (*2*). Although HER2-targeted therapies can improve survival, resistance to these therapies often occurs (*3*). Moreover, these agents are ineffective against brain metastases, an increasingly prevalent and lethal consequence of HER2-positive breast cancer (*4*). For these reasons, targeted therapies with different mechanisms of action and suitable for delivery to disease within the brain are urgently needed.

Targeted α-particle therapy (TAT) has emerged as an attractive strategy for cancer treatment and exerts its cytotoxic effects through different mechanisms (*5*) than currently approved HER2-targeted drugs. Moreover, their 50-100 μm tissue range in combination with their high cytotoxicity make α-particles of promise for irradiation of metastases while minimizing toxicity to surrounding normal tissues. This provided motivation for labeling HER2-targeted antibodies with a variety of α-emitters and evaluating their therapeutic potential in animal models (*6-9*) and in patients (*10*). Although some encouraging results were reported, the large size of intact antibodies led to slow and inhomogeneous delivery to tumor and prolonged residence time in normal tissues (*11*).

To circumvent these limitations, single-domain antibody fragments (sdAbs; aka nanobodies or VHH) are being evaluated as an alternative scaffold for TAT with HER2 being perhaps the most widely investigated molecular target (*11,12*). Derived from Camelids, these 12-15 kDa proteins can have nanomolar or sub-nanomolar affinity and exhibit low immunogenicity (*13*). Importantly, preclinical studies have demonstrated the considerably more rapid tumor penetration of sdAbs compared with intact antibodies (*14*)

as well as their successful delivery to HER2-positive brain tumors (*15*). The feasibility of labeling HER2 Domain I targeted 2Rs15d with the α-emitters ^{225}Ac (*16*) and ^{213}Bi (*17*) has been reported. While tumor targeting was demonstrated, high renal uptake also was observed.

On the other hand, labeling this anti-HER2 sdAb with the α-emitting radiohalogen ^{211}At resulted in much more favorable tumor-to-kidney ratios (*18*). Moreover, ^{211}At has a half-life (7.2 h) that is well-matched to the pharmacokinetics of sdAbs in humans (*19*). Astatine-211 has other attractive features for TAT including emitting only one α-particle per decay, lack of confounding α-particle recoil effects, and increasing availability at a reasonable cost (*20*).

Our previous studies have shown that synergizing the characteristics of the ^{211}At-labeled prosthetic agent and the anti-HER2 sdAb can provide excellent tumor targeting (*21*). Herein, we evaluate the therapeutic efficacy of these ^{211}At-labeled sdAb conjugates and demonstrate a durable dose-dependent therapeutic effect after a single dose in a subcutaneous breast carcinoma xenograft model.

MATERIALS AND METHODS

General

Details about general procedures including cell culture and the sources for materials used in these experiments are presented in the Supplemental Materials (*20,22,23*).

sdAbs

The characteristics of the anti-HER2 sdAbs 5F7 and VHH_1028, both reacting with the trastuzumab HER2 binding site, have been described previously (*24, 25*). A HER2-

irrelevant control, VHH_2001 was constructed by combining the framework amino acid sequences of these anti-HER2 sdAbs (same for both) with the CDR sequences from green fluorescent protein (GFP) specific sdAb cAbGFP4 (*26*). All sdAbs were produced by ATUM (Newark, CA) using their known amino acid sequences as described (*25*).

Radiosynthesis and Quality Control of *iso*-^{211}At-SAGMB-sdAb conjugates

The synthesis of *iso*-^{211}At-SAGMB was modified for higher ^{211}At radioactivity level labeling based on a previously published method (*21*). Astatine-211 in NCS/methanol (~370 MBq) was added to a vial containing 150 µg of Boc_2-SGMTB precursor followed by 4 µL acetic acid. The reaction mixture was vortexed and incubated at room temperature for 30 min. Methanol was evaporated with a gentle stream of nitrogen; to ensure its complete removal, addition of 100 µL of ethyl acetate and its evaporation was performed twice. The residue was reconstituted with 100 µL of 30% (v/v) ethyl acetate in hexanes, and Boc_2-*iso*-^{211}At-SAGMB was isolated by normal phase HPLC (two 50 µL injections). For both runs, the HPLC fractions containing Boc_2-*iso*-^{211}At-SAGMB were pooled and the solvents were evaporated under a stream of argon. Boc protecting groups were removed by treatment of each reaction vial with 100 µL of trifluoroacetic acid at room temperature for 10 min. To insure complete removal of trifluoroacetic acid, ethyl acetate addition (100 µL) and its evaporation was performed three times. A solution of the sdAb (5F7, VHH_1028, or VHH_2001) in 0.1 M borate buffer (pH=8.5, 50 µL, 2 mg/mL) was added to the vial containing *iso*-^{211}At-SAGMB and the mixture was incubated at room temperature for 20 min. *Iso*-^{211}At-SAGMB-sdAb conjugates were purified by gel filtration using a PD-10 column eluted with phosphate buffered saline (PBS) as described (*21*).

The *iso*-^{211}At-SAGMB-sdAbs were evaluated by SDS-PAGE and in some cases, gel-permeation HPLC (GPC) as described in Supplemental Material. Target binding fractions were determined using HER2-coated beads (*24*) but following a modified procedure recently developed (*27*). The HER2 binding affinities of therapeutic batches of *iso*-^{211}At-SAGMB-5F7 and *iso*-^{211}At-SAGMB-VHH_1028 were determined on BT474 cells as described previously (*23*).

***In Vitro* Experiments**

Cell Uptake and Internalization Kinetics. The internalization rate constant (k_e) and the washout rate constant (k_x) for *iso*-^{211}At-SAGMB-5F7 were determined as reported previously (*28*). Briefly, BT474 cells (8×10^5 cells/well/3 mL medium) in 6-well plates were incubated overnight at 37°C. Medium was removed and replenished with fresh medium containing 1 nmol of *iso*-^{211}At-SAGMB-5F7 and the fraction of unbound, surface-bound and internalized ^{211}At activity after incubation at 37°C for 1, 2, 3, 4, 5, and 6 h was determined as described (*23,24*). Nonspecific binding, determined in parallel by coincubation with a 100-fold molar excess of trastuzumab, was minimal. A similar format was used to determine the washout rate constant k_x by measuring the loss of internalized ^{211}At activity as a function of time. The internalization process was assumed to be linear and the internalization rate constant k_e was expressed as $k_e \times t_{in} = m_i/m_{b,}$ where t_{in} is the incubation time, m_i is the internalized fraction and m_b is the surface bound fraction. Rate constants were then calculated as described (*28*).

Cell Survival Assay. The cytotoxicity of *iso*-^{211}At-SAGMB-5F7 and HER2-unreactive *iso*-^{211}At-SAGMB-VHH_2001 were compared on BT474 cells in a colony forming assay as described in Supplemental Materials (*29*).

In Vivo Experiments

Animal Procedures. Animal studied conformed to protocols approved by the Duke University Animal Care and Use Committee for compliance with the National Institutes of Health for use of laboratory animals.

Biodistribution. Four-week-old female athymic mice (25 g; Jackson Labs) received subcutaneous implants of estrogen pellets (17β-estradiol, 0.72 mg) in the neck. Subcutaneous BT474 xenografts were established 2 days later by shoulder inoculation of 20×10^6 BT474 cells in 1:1 (v/v) Matrigel® in tissue culture medium (100 µL). When tumors reached ~250 mm^3, animals received *iso*-^{211}At-SAGMB-VHH_1028 (200 kBq/1 µg, 100 µL PBS) via intravenous injection. Groups of 5 mice were killed by isoflurane overdose 1, 4, and 21 h after injection, and necropsied. Tumor and normal tissues were harvested and counted for ^{211}At activity using an automated gamma counter. Results were expressed as percent injected dose (%ID) per organ and per gram of tissue (%ID/g). The biodistribution of HER2-irrelevant *iso*-^{211}At-SAGMB-VHH_2001 (130 kBq/1 µg) was evaluated in the same way. Finally, a paired-label study directly compared the tissue distribution of *iso*-^{125}I-SGMIB-5F7 and *iso*-^{131}I-SGMIB-VHH_1028 in athymic mice bearing subcutaneous HER2-expressing SKOV-3 xenografts generated as described (*25*). Animals received approximately 175 kBq (1 µg) of both radioiodinated anti-HER2 sdAbs, and groups of 5 mice were necropsied at 1, 4, and 24 h after injection. For each animal, the ^{131}I-to-^{125}I tumor uptake ratio was determined and differences in *iso*-^{131}I-SGMIB-VHH_1028 and *iso*-^{125}I-SGMIB-5F7 tumor accumulation were analyzed for statistical significance using a paired *t*-test.

Radiation Dosimetry. From the *iso*-^{211}At-SAGMB-VHH_1028 biodistribution data, areas under the time activity curves were calculated by trapezoidal integration using GraphPad Prism. These were multiplied by the mean energy per ^{211}At transition ($4x10^{-13}$ Gy kg/Bq s) and ^{211}Po daughter ($1.2x10^{-12}$ Gy kg/Bq s), corrected for the branching ratio. The absorbed dose was calculated using a radiation weighting factor of 5 for α-particles as recommended (*30*) and expressed as Sv/MBq.

Antitumor efficacy. In the first experiment (Detailed in Supplemental Table 1), the therapeutic efficacy of *iso*-^{211}At-SAGMB-5F7 was evaluated in NOD-*scid*-IL2Rgamma^{null} (NSG; Jackson Labs) mice with subcutaneous BT474 xenografts generated as described previously (*23*). Tumor growth was monitored twice a week and tumor volume was calculated as volume=length×width^2×0.52. When tumor volumes reached 150-300 mm^3, mice were randomized into 4 groups and injected *i.v.* with PBS (n=10) or 0.7 (n=4), 1.9 (n=6), or 3 MBq (n=4) of *iso*-^{211}At-SAGMB-5F7 (3-14 µg sdAb). Animals were monitored for 182 days as described below.

In the second experiment (Detailed in Supplemental Table 2), groups of 10-12 female athymic mice with ~180 mm^3 subcutaneous BT474 xenografts generated as described above were injected intravenously with 1, 1.9 or 3 MBq, of *iso*-^{211}At-SAGMB-VHH_1028 in 100 µL PBS or PBS alone and monitored for 205 days.

In the third experiment (Detailed in Supplemental Table 3), the specificity of the therapeutic effect was investigated in female athymic mice bearing BT474 xenografts. After estrogen pellet implantation (17β-estradiol, 0.72 mg), mice were supplied with ascorbic acid (240 mg/L) and citric acid (1 g/L) in their drinking water to prevent urolithiasis. Mice with ~120 mm^3 tumors were randomized into 3 groups, and injected *i.v.*

with 1.0 MBq of *iso*-^{211}At-SAGMB-VHH_1028 (n=11, 3 μg), 1.1 MBq of *iso*-^{211}At-SAGMB-VHH_2001 (n=11, 3.7 μg), or PBS (n=10). Animals were monitored for 196 days.

In these experiments, mice were euthanized if any of the following occurred: 1) tumor volume >1000 mm^3, 2) body weight loss >20%, 3) tumor ulceration or necrosis, or 4) any other health conditions that necessitated euthanasia per Duke IACUC policy. Deceased animals were necropsied to determine cause of death.

Statistics

Data are presented as mean ± standard deviation. Methods for statistical and data analysis of the therapeutic efficacy studies ae described in the Supplemental Materials.

RESULTS

Radiosynthesis and Quality Control of *iso*-^{211}At-SAGMB-sdAb conjugates

In previous studies performed with 30-56 MBq ^{211}At activity**,** Boc$_2$-*iso*-^{211}At-SAGMB was synthesized with 66.8 ± 2.4% average yield in ~4 h (*21*). The procedure was optimized for ~370 MBq ^{211}At reactions by varying the reaction volume, reaction time, acetic acid level and normal-phase HPLC column injection volume. The Boc$_2$-*iso*-^{211}At-SAGMB radiochemical yield (RCY) was lower for ~370 MBq ^{211}At reactions, 31.0 ± 7.1% (n=10); the radiochemical purity (RCP) determined by normal-phase HPLC was >99%. Deprotection of Boc$_2$-*iso*-^{211}At-SAGMB to generate *iso*-^{211}At-SAGMB was almost quantitative with a maximum of 222 MBq of *iso*-^{211}At-SAGMB being produced. Conjugation of *iso*-^{211}At-SAGMB to sdAbs proceeded in 51.9 ± 14.7% (n=9) RCY with no significant differences observed among 5F7, VHH_1028 and VHH_2001. The total synthesis time for producing these *iso*-^{211}At-SAGMB-sdAb conjugates from initial ^{211}At

activity was 3.5 h with an overall radiochemical yield of 16.1 ± 7.0%. A typical synthesis starting from 370 MBq ^{211}At provided ~74 MBq of ^{211}At-labeled sdAb. The molar activity for the *iso*-^{211}At-SAGMB-sdAbs was 1.74-4.41 MBq/nmole.

SDS-PAGE/phosphor imaging of the *iso*-^{211}At-SAGMB-sdAbs revealed a single radioactive band corresponding to the expected molecular weight of ~13 kDa (Supplemental Fig. 1) with a RCP of 97.6 ± 0.8% (n=9). The RCP of 4 batches of *iso*-^{211}At-SAGMB-VHH_1028 also was evaluated by GPC (Supplemental Fig. 2), which indicated a single peak at the expected retention time and a RCP of 98.6 ± 1.0%. The target binding fraction of *iso*-^{211}At-SAGMB-5F7 was 84.3% (n=2) and 87.1% (n=1) for *iso*-^{211}At-SAGMB-VHH_1028. No HER2 binding was observed for the HER2-irrelevant *iso*-^{211}At-SAGMB-VHH_2001 control. Saturation binding assays on HER2-expressing BT474 breast cancer cells performed with therapy-level batches of *iso*-^{211}At-SAGMB-5F7 and *iso*-^{211}At-SAGMB-VHH_1028 gave K_d values of 4.49 ± 0.39 nM and 3.87 ± 0.88 nM, respectively (Supplemental Fig. 3).

In Vitro **Experiments**

Internalization and Expulsion Rate. In order to quantify the rate of internalization of *iso*-^{211}At-SAGMB-5F7, the ratio between internalized and surface bound ^{211}At activity was plotted as a function of incubation time (Supplemental Fig. 4). A linear regression was run to give k_e = (3.79 ± 0.29) × 10^{-5} (s^{-1}) (95% confidence interval: R^2=0.9155). The rate constant for ^{211}At loss (expulsion; k_x), was determined in similar fashion based on a wash-out kinetics assay. Expulsion of radioactivity was not observed during the 4-h experimental period as the ratio of m_i/m_b increased; thus, k_x was considered to be 0.

Cell Survival Assay. The survival fraction of HER2-positive BT474 breast carcinoma cells after incubation with varying activity concentrations of *iso*-^{211}At-SAGMB-5F7 prepared at 3.9 MBq/nmole is given in Fig.1. The D_0 (activity concentration to reduce survival to 37%) was determined to be 1.313 kBq/mL for *iso*-^{211}At-SAGMB-5F7. The cytotoxicity of the *iso*-^{211}At-SAGMB-VHH_2001 control was measured in parallel and no reduction in survival was observed (Fig.1) demonstrating that the cytotoxicity of *iso*-^{211}At-SAGMB-5F7 was HER2 specific.

***In Vivo* Experiments**

Biodistribution and dosimetry. The tissue distribution of *iso*-^{131}I-SGMIB-VHH_1028 in NSG mice with BT474 xenografts was reported previously (*21*). The biodistribution of *iso*-^{211}At-SAGMB-VHH_1028 in athymic mice with subcutaneous BT474 xenografts is summarized in Fig. 2. The tumor uptake of *iso*-^{211}At-SAGMB-VHH_1028 was 10.28 ± 0.90% ID/g at 1 h and 10.21 ± 3.10% ID/g at 4 h and decreased to 4.00 ± 1.90% ID/g at 21 h. Rapid clearance of radioactivity from normal organs was observed. The highest ^{211}At levels were seen in the kidneys, which decreased from 34.20 ± 13.63% ID/g at 1 h to 4.46 ± 0.62% ID/g at 4 h. Thyroid activity levels ranged from 0.53 ± 0.25% at 4 h to 0.38 ± 0.17% at 21 h (Supplemental Table 4) consistent with only minor dehalogenation *in vivo*. Tumor uptake of HER2-irrelevant *iso*-^{211}At-SAGMB-VHH_2001 was 3.17 ± 0.50% ID/g, 2.05 ± 0.23% ID/g, and 0.58 ± 0.58% ID/g (Supplemental Table 5) at 1, 4 and 21 h, respectively, values 3.2, 5.0 and 7.7 times lower than those for *iso*-^{211}At-SAGMB-VHH_1028. The biodistribution of co-administered *iso*-^{131}I-SGMIB-VHH_1028 and *iso*-^{125}I-SGMIB-5F7 in athymic mice with SKOV-3 xenografts is summarized in Supplemental Table 6. With few exceptions, normal tissue levels for the two sdAbs were not significantly

different. In tumor, ^{131}I-to-^{125}I uptake ratios were not significantly different from unity (1.07 ± 0.20 at 1 h, 0.99 ± 0.01 at 4 h and 0.91 ± 0.10 at 24 h) confirming equivalent tumor localizing capacity for the 5F7 and VHH_1028 *iso*-SGMIB conjugates.

Radiation absorbed doses calculated from the *iso*-^{211}At-SAGMB-VHH_1028 biodistribution data are presented in Table 1 both per MBq and for 3.0 MBq, the highest ^{211}At activity evaluated in the therapeutic efficacy experiments. The tumor absorbed dose was estimated to be 14.4 Sv/MBq, which was higher than that calculated for all normal tissues except the kidneys (14.6 Sv/MBq). At 3.0 MBq, the tumor was estimated to have received a radiation dose of 43.3 Sv. The tumor absorbed dose for *iso*-^{211}At-SAGMB-VHH_2001 was estimated to be 3.08 Sv/MBq, 4.7 times lower than that for *iso*-^{211}At-SAGMB-VHH_1028.

Antitumor Efficacy. The first experiment evaluated the therapeutic potential of *iso*-^{211}At-SAGMB-5F7 in NSG mice with BT474 xenografts; tumor volumes at treatment and dosing details are summarized in Supplemental Table 1. A dose-dependent tumor growth delay was observed (Fig. 3A) - tumor growth was significantly delayed for the 3.0 MBq group (P<0.0001), to a degree that was significantly greater than in the 1.9 MBq (P=0.0001) and 0.7 MBq (P<0.0001) groups. A maximum tumor growth inhibition of >50% was observed in 1 of 4 mice in 0.7 MBq group, 5 of 6 in the 1.9 MBq group and all 4 in 3.0 MBq group, both the 1.9 and 3.0 MBq groups having 3 mice with no detectable tumors (Fig. 3B). A significant survival benefit was seen for the treatment groups (P<0.0001) with a median survival of 29 d for the control group, and 105.5, 126.5, and 143.5 d for the 0.7, 1.9 and 3.0 MBq groups, respectively (Fig. 3C). No

significant differences in body weight (Fig. 3D) or other clinically observable signs of toxicity were seen between the treatment and control groups.

Tumor volumes at treatment and dosing details for the single-dose *iso*-^{211}At-SAGMB-VHH_1028 therapy study in athymic mice with BT474 xenografts are summarized in Supplemental Table 2. Significant tumor growth delay was observed in all treatment groups (P<0.0001), which was dose dependent (P=0.0011 for 3.0 *vs.* 1.9 MBq doses; P<0.0001 for 3.0 vs. 1.0 MBq doses) (Fig. 4A). However, the therapeutic responses were not significantly different for the 1.0 vs. 1.9 MBq doses. A single dose of *iso*-^{211}At-SAGMB-VHH_1028 resulted in the complete regression of tumors in 8 of 11 mice receiving 3.0 MBq, 3 of 12 mice receiving 1.9 MBq, and 3 of 10 mice receiving 1.0 MBq, with >50% tumor volume regression seen in 11 of 11, 10 of 12, and 7 of 10 animals receiving the 3.0, 1.9 and 1.0 MBq doses, respectively (Fig. 4B). Significant survival benefit (P<0.0001 from Mantel-Cox and Gehan-Breslow-Wilcoxon tests) was observed for all treatment groups. A single dose of *iso*-^{211}At-SAGMB-VHH_1028 increased the median survival from 50.5 d (control group) to 209 d (3.0 MBq group) (Fig. 4C). No significant differences in body weight (Fig. 4D) or other clinically observable signs of toxicity were seen between the treatment and control groups.

The third therapy study was designed to evaluate the specificity of the *iso*-^{211}At-SAGMB-VHH_1028 therapeutic effect by direct comparison to the HER2-unreactive *iso*-^{211}At-SAGMB-VHH_2001 control. A Spaghetti plot of individual mouse tumor volumes (Fig. 5A) and a waterfall plot of maximum tumor response (Fig. 5B) indicate significant tumor growth delay for the HER2-specific *iso*-^{211}At-SAGMB-sdAb conjugate with 6 of 11 mice showing >50% tumor regression and 4 mice showing no evidence of tumor at the

1.0 MBq dose. In contrast, no tumor growth delay was seen in animals receiving the *iso*-^{211}At-SAGMB-sdAb control. As shown in Fig. 5C, no significant difference was observed between the median survival of the PBS group (44 d) and the *iso*-^{211}At-SAGMB-sdAb control (34 d). A clear survival benefit was seen for the HER2-specific *iso*-^{211}At-SAGMB-VHH_1028 conjugate with a median survival of 159 d vs. 44 d for the PBS group (P<0.0001; Mantel-Cox and Gehan-Breslow-Wilcoxon tests). No significant differences in body weight (Fig 5D) or other clinically observable signs of toxicity were seen between the treatment and control groups.

DISCUSSION

Because of their rapid and homogeneous tumor penetration (*14*), sdAbs have emerged as an attractive vehicle for TAT (*12*). In the present study, we have demonstrated dramatic tumor control could be achieved in a HER2-expressing subcutaneous model of breast cancer after a single-dose of ^{211}At-labeled HER2-targeted sdAbs. Astatine-211 is ideally suited for labeling sdAbs because its 7.2-h half-life is well matched to the ~8 h biologic clearance half-life of labeled sdAbs in humans (*19*). Moreover, in studies where the same sdAb was labeled with different α-emitters, kidney activity levels were considerably lower for ^{211}At (*18*) compared with ^{213}Bi (*17*) and ^{225}Ac (*16*) suggesting that an additional benefit in selecting ^{211}At for labeling sdAbs is the lower risk of renal toxicity. Other more generalizable advantages of ^{211}At for TAT include the emission of only 1 α-particle per decay, absence of α-emitting daughters, and improved availability at a reasonable cost (*20*).

Herein we have evaluated a TAT development strategy for HER2-expressing cancers: combining the best currently available ^{211}At residualizing agent - *iso*-^{211}At-SAGMB (*21*) –

with HER2-specific sdAbs with high affinity and internalization - properties that should enhance and prolong tumor uptake of these small proteins (*31*). For anti-HER2 sdAbs, initial studies utilized 5F7, which has a HER2 binding affinity of 0.2 nM (*32*) and exhibited excellent uptake in BT474 cells and xenografts after labeling with *iso*-^{211}At-SAGMB (*21*). VHH_1028 also binds to a trastuzumab-competitive HER2 site with 0.2 nM affinity (*25*). A head-to-head comparison using ^{131}I-SGMIB-5F7 and ^{131}I-SGMIB-VHH_1028 confirmed that the two sdAbs cross compete for the same HER2 epitope and bind to BT474 cells with nearly identical characteristics (Supplemental Fig. 5).

The binding affinities determined on BT474 cells for *iso*-^{211}At-SAGMB-5F7 and *iso*-^{211}At-SAGMB-VHH_1028 were 4.49 ± 0.39 nM and 3.87 ± 0.88 nM, respectively. The *iso*-^{211}At-SAGMB-5F7 affinity was somewhat higher than measured previously (3.0 nM) at lower ^{211}At activities (*21*) but still suitable for TAT. Regarding internalization, the internalization rate and lack of measurable expulsion of *iso*-^{211}At-SAGMB-5F7 were in excellent agreement with those measured previously on BT474 cells for trastuzumab (*28*). Thus, the cellular residence time for *iso*-^{211}At-SAGMB-5F7 should be compatible with effective cell killing. Indeed, the cytotoxicity of *iso*-^{211}At-SAGMB-5F7 (D_0=1.313 kBq/mL) was higher than that determined for ^{211}At-trastuzumab (1.7 kBq/mL) under similar conditions on the same BT474 cell line (*28*).

Therapeutic responses after ^{211}At-trasuzumab treatment have been observed in various animal models; however, except for a recent study (*33*), these have involved direct delivery into a tumor-compromised compartment (*6,34*). After intrathecal delivery, regional differences in therapeutic effectiveness against carcinomatous meningitis were observed with ^{211}At-trasuzumab suggesting inhomogeneous distribution of the labeled

mAb had occurred (*6*). In addition, a recent study has demonstrated that unlike trastuzumab, sdAbs can be delivered to HER2-positive brain metastases (*35*) for which better treatments are urgently needed (*4*). Thus, a ^{211}At-labeled sdAb with trastuzumab-like binding and internalization properties but capable of more homogeneous delivery might be advantageous, provided that the delivery of therapeutically relevant levels to tumor could be achieved.

Based on the biodistribution of *iso*-^{211}At-SAGMB-VHH_1028 in athymic mice, a tumor dose of 14.4 Sv/MBq was calculated, which is higher than that reported (4.58 Gy/MBq) for ^{211}At-trastuzumab in a gastric-cancer-liver-metastases model (*33*). We note that the BT474 tumor targeting (and kidney uptake) of *iso*-^{211}At-SAGMB-VHH_1028 determined in athymic mice were lower than those reported previously for *iso*-^{211}At-SAGMB-5F7 in NSG mice bearing the same xenograft (*21*). Given the similar properties of the two VHH, this behavior likely reflects animal model-dependent differences in distribution. Consistent with this, the BT474 tumor and kidney uptake of *iso*-^{131}I-SGMIB-5F7 were lower in athymic mice (*32,36*) than in NSG mice (*21*). An additional experiment was performed to confirm that differences in the biodistribution of *iso*-^{211}At-SAGMB-5F7 and *iso*-^{211}At-SAGMB-VHH_1028 reflected the influence of the mouse strain. A paired-label study in athymic mice bearing HER2-expressing SKOV-xenografts demonstrated essentially identical tumor uptake of *iso*-^{125}I-SGMIB-5F7 and *iso*-^{131}I-SGMIB-VHH_1028 (Supplemental Table 6).

Although different animal models and sdAbs were used, the therapeutic efficacy of other α-emitter-anti-HER2 sdAb conjugates has been evaluated and can serve as benchmarks for comparison. Using an intracranial SKOV3.IP1 ovarian tumor model, 3

weekly doses of ^{225}Ac-2Rs15d increased median survival by 35% (6 d) (*35*). Administration of 3 doses of ^{213}Bi-2Rs15d to mice with intraperitoneal SKOV3.IP1 tumors increased median survival by 51% and 26% at doses of 0.5 MBq and 1.0 MBq, respectively (*17*). Although gelofusine was co-administered to reduce renal retention, the kidney radiation dose from ^{213}Bi-2Rs15d was 6 times higher than that to tumor (*17*), likely limiting dose escalation.

The therapeutic responses we observed after a single dose of *iso*-^{211}At-SAGMB-VHH_1028 in the BT474 breast carcinoma model are thus quite encouraging. Notably, even at the lowest dose level investigated (1.0 MBq), median survival was increased by 361%, from 44 d to 159 d (Fig. 5C), with 4 of 11 animals having complete tumor regression, while no significant survival prolongation was observed with the HER2-irrelevant ^{211}At-sdAb control. Importantly, these responses were obtained at ^{211}At activity that would deliver only 14.6 Sv to the kidneys (Table 1). Although radiation toxicity thresholds for TAT are not well defined, this dose is well below the 23 Gy benchmark threshold for renal toxicity for conventional external beam radiation for which 1 Gy = 1 Sv. Finally, these results further confirm the potential advantages of TAT for cancer treatment – a single dose of *iso*-^{211}At-SAGMB-VHH_1028 was considerably more effective than 4 weekly doses of the analogous β-emitting *iso*-^{131}I-SGMIB-VHH_1028 conjugate in the same BT474 xenograft model (*25*).

Because VHH_1028 lacks the CDR2 lysine present in 5F7, VHH_1028 might be better suited for patient therapy-level labeling. However, a recent study using SPR analysis demonstrated full retention of affinity for 1:1 *iso*-SGMIB-5F7 conjugate(K_D=0.21 nM vs. 0.22 nM for unmodified 5F7 run in parallel) (*36*), suggesting that either the CDR2 lysine

was not reactive for conjugation or its modification did not alter HER2 binding. With ^{211}At at a 1:1 prosthetic agent:5F7 substitution level, this would be equivalent to 1221 GBq/mg. Even if the protein dose for an ^{211}At-5F7 therapy was limited to 50 μg, the dose administered to patients in a recent ^{131}I-labeled anti-HER2 sdAb imaging study (*19*), this would be equivalent to 61 GBq (~1,650 mCi) of ^{211}At, an activity level far exceeding a feasible patient therapy dose. Thus, the CDR2 lysine in 5F7 should not compromise ^{211}At labeling at therapeutically relevant activities, suggesting that both 5F7 and VHH_1028 are excellent candidates for development as ^{211}At-labeled radiopharmaceuticals for treating HER2-expressing cancers.

A limitation of this study is that it did not include histopathological analysis of acute and long-term radiotoxicity, and determination of the maximum tolerated dose. Given the lack of clinically observable toxicities at the highest dose investigated and a median survival greater than 6 months, it might be possible to achieve even better single dose tumor response at a higher activity level. A long-term radiotoxicity study is planned that will include histopathological analysis and evaluation of blood chemistry as we have done for other ^{211}At-labeled TAT agents (*37*). This will provide critical information for designing future dose escalation experiments and hopefully, for clinical translation of these ^{211}At-SAGMB-HER2-targeted sdAb conjugates.

CONCLUSION

TAT with single doses of *iso*-^{211}At-SAGMB-anti-HER2-sdAb conjugates resulted in significant tumor growth delay and survival prolongation in a murine model of HER2-expressing breast cancer with no apparent normal tissue toxicities. This TAT strategy

warrants further consideration for the treatment of patients with HER2-expressing cancers.

DISCLOSURE

Financial support was received from CA42324 and Cereius, Inc. Ganesan Vaidyanathan and Michael Zalutsky are shareholders in Cereius and are entitled to royalty distributions from Cereius related to the radiolabeling technologies described herein. No other potential conflicts of interest relevant to this article exist.

KEY POINTS

QUESTION: Are ^{211}At-labeled sdAb conjugates candidates for targeted α-particle therapy of HER2-expressing cancers?

PERTINENT FINIDINGS: ^{211}At-labeled sdAbs targeting Domain IV of HER2 controlled tumor growth and prolonged survival at single doses of 0.7-3.0 MBq without toxicity while a ^{211}At-labeled HER2-irrelevant sdAb was ineffective.

IMPLICATIONS FOR PATIENT CARE: Because of their considerable therapeutic effects with minimal normal tissue toxicity, these *iso*-^{211}At-SAGMB-sdAb conjugates could provide an attractive therapeutic option for patients who do not respond to conventional HER2-targeted therapies.

REFERENCES

1. Oh D-Y, Bang Y-J. HER2-targeted therapies—a role beyond breast cancer. *Nature Rev Clin Oncol.* 2020;17:33-48.

2. Slamon DJ, Leyland-Jones B, Shak S, et al. Use of chemotherapy plus a monoclonal antibody against HER2 for metastatic breast cancer that overexpresses HER2. *N Engl J Med.* 2001;344:783-792.

3. Pernas S, Tolaney SM. HER2-positive breast cancer: new therapeutic frontiers and overcoming resistance. *Ther Adv Med Oncol.* 2019;11:1758835919833519.

4. Hosonaga M, Saya H, Arima Y. Molecular and cellular mechanisms underlying brain metastasis of breast cancer. *Cancer Met Rev.* 2020;39:711-720.

5. Pouget J-P, Constanzo J. Revisiting the radiobiology of targeted alpha therapy. *Front Med.* 2021;8:692436.

6. Boskovitz A, McLendon RE, Okamura T, Sampson JH, Bigner DD, Zalutsky MR. Treatment of HER2-positive breast carcinomatous meningitis with intrathecal administration of α-particle-emitting ^{211}At-labeled trastuzumab. *Nucl Med Biol.* 2009;36:659-669.

7. Milenic DE, Garmestani K, Dadachova E, et al. Targeting of HER2 antigen for the treatment of disseminated peritoneal disease. *Clin Cancer Res.* 2004;10:7834-7841.

8. Borchardt PE, Yuan RR, Miederer M, McDevitt MR, Scheinberg DA. Targeted actinium-225 in vivo generators for therapy of ovarian cancer. *Cancer Res.* 2003;63:5084-5090.

9. Wickstroem K, Karlsson J, Ellingsen C, et al. Synergistic effect of a HER2 targeted thorium-227 conjugate in combination with Olaparib in a BRCA2 deficient xenograft model. *Pharmaceuticals.* 2019;12:155.

10. Meredith R, Torgue J, Shen S, et al. Dose escalation and dosimetry of first-in-human α radioimmunotherapy with ^{212}Pb-TCMC-trastuzumab. *J Nucl Med.* 2014;55:1636-1642.

11. Altunay B, Morgenroth A, Beheshti M, et al. HER2-directed antibodies, affibodies and nanobodies as drug-delivery vehicles in breast cancer with a specific focus on radioimmunotherapy and radioimmunoimaging. *Eur J Nucl Med Mol Imaging* 2021:48:1371-1389.

12. Dekempaneer Y, Keyaerts M, Krasniqi A, et al. Targeted alpha therapy using short-lived alpha-particles and the promise of nanobodies as targeting vehicle. *Expert Opin Biol Ther.* 2016;16:1035-1047.

13. Piramoon M, Khodadust F, Hosseinimehr SJ. Radiolabeled nanobodies for tumor targeting: From bioengineering to imaging and therapy. *Biochim Biophys Acta Rev Cancer*. 2021;1875:188529.

14. Debie P, Lafont C, Defrise M, et al. Size and affinity kinetics of nanobodies influence targeting and penetration of solid tumors. *J Control Release.* 2020;317:34-42.

15. Zhou Z, Vaidyanathan G, McDougald D, et al. Fluorine-18 labeling of the HER2-targeting single-domain antibody 2Rs15d using a residualizing label and preclinical evaluation. *Mol Imag Biol.* 2017;19:867-877.

16, Pruszynski M, D'Huyvetter M, Bruchertseifer F, Morgenstern A, Lahoutte T. Evaluation of an antiHER2 nanobody labeled with ^{225}Ac for targeted α-particle therapy of cancer. *Mol Pharmaceutics.* 2018;15:1457-1466.

17. Dekempeneer Y, Caveliers V, Ooms M, et al. Therapeutic efficacy of ^{213}Bi-labeled sdAbs in a preclinical model of ovarian cancer. *Mol Pharmaceutics.* 2020;17:3553-3566.

18. Dekempeneer Y, Back T, Aneheim E, et al. Labeling of anti-HER2 nanobodies with astatine-211: optimization and the effect of different coupling reagents on their *in vivo* behavior. *Mol Pharmaceutics.* 2019;16:3524-3533.

19. D'Huyvetter M, Vos J, Caveliers V, et al. Phase I trial of ^{131}I-GMIB-Anti-HER2-VHH1, a new promising candidate for HER2-targeted radionuclide therapy in breast cancer patients. *J Nucl Med.* 2021;62:1097-1105.

20. Feng Y, Zalutsky MR. Production, purification and availability of ^{211}At: near term steps towards global access. *Nucl Med Biol.* 2021;100-101:12-23.

21. Choi J, Vaidyanathan G, Koumarianou E, Kang CM, Zalutsky MR. Astatine-211 labeled anti-HER2 5F7 single domain antibody fragment conjugates: Radiolabeling and preliminary evaluation. *Nucl Med Biol.* 2018;56:10-20.

22. Pozzi O, Zalutsky MR. Radiopharmaceutical chemistry of targeted radiotherapeutics III: part 3: α-particle-induced radiolytic effects on the chemical behavior of ^{211}At. *J Nucl Med.* 2007;48:1190-1196.

23. Pruszynski M, Koumarianou E, Vaidynathan G, et al. Improved tumor targeting of anti-HER2 nanobody through *N*-succinimidyl 4-guanidinomethyl-3-benzoate radiolabelling. *J Nucl Med.* 2014;55:650-656.

24. Pruszynski M, Koumarianou E, Vaidynathan G, et al. Targeting breast carcinoma with radioiodinated antiHER2 nanobody. *Nucl Med Biol.* 2013;40:52-59.

25. Feng Y, Meshaw R, McDougald D, et al. Evaluation of an ^{131}I-labeled HER2-specific single domain antibody fragment for the radiopharmaceutical therapy of HER2-expressing cancers. *Scientific Reports* 2022;12:3020.

26. Saerens D, Pellis M, Loris R, et al. Identification of a universal VHH framework to graft non-canonical antigen-binding loops of camel single-domain antibodies. *J Mol Biol.* 2005;352:597-6607.

27. Sharma SK, Lyashchenko SK, Park HA, et al. A rapid bead-based radioligand binding assay for the determination of target-binding fraction and quality control of radiopharmaceuticals. *Nucl Med Biol.* 2019;71:32-38.

28. Akabani G, Carlin S, Welsh P, Zalutsky MR. In vitro cytotoxicity of ^{211}At-labeled trastuzumab in human breast cancer cell lines: effect of specific activity and HER2 receptor heterogeneity on survival fraction. *Nucl Med Biol.* 2006;33:333-347.

29. Kiess A, Minn I, Vaidyanathan G, et al. (2S)-2-(3-(1-carboxy-5-(4-^{211}At-astatobenzamido)pentyl)ureido)-pentanedioic acid for PSMA-targeted α-particle radiopharmaceutical therapy. *J Nucl Med.* 2016;57:1569-1575.

30. Sgouros G, Roeske JC, McDevitt MR, et al. MIRD Pamphlet No.22: radiobiology and dosimetry of alpha-particle emitters for targeted radionuclide therapy. *J Nucl Med.* 2010;51:311-328.

31. Schmidt MM, Wittrup KD. A modeling analysis of the effects of molecular size and binding affinity on tumor targeting. *Mol Cancer Ther.* 2009;8:2861-2871.

32. Zhou Z, Meshaw R, Zalutsky MR, Vaidyanathan G. Site-specific and residualizing linker for ^{18}F labeling with enhanced renal clearance: application to anti-HER2 single-domain antibody fragment. *J Nucl Med.* 2021;62:1624-1630.

33. Li HK, Morokoshi Y, Kodaira S, et al. Utility of ^{211}At-trastuzumab for the treatment of metastatic gastric cancer in the liver: evaluation of a preclinical α-radioimmunotherapy approach in a clinically relevant mouse model**.** *J Nucl Med.* 2021;62:1468-1474.

34. Palm S, Back T, Claesson I, et al. Therapeutic efficacy of astatine-211-labeled trastuzumab on radioresistant SKOV-3 tumors in nude mice. *Int J Radiat Oncol Biol Phys.* 2007;69:572-579.

35. Puttemans J, Dekempeneer Y, Eersels JL, et al. Preclinical targeted α- and β-radionuclide therapy in HER2-positive brain metastasis using camelid single-domain antibodies. *Cancers* 2020:12:1017.

36. Feng Y, Zhou Z, McDougald D, Meshaw RL, Vaidyanathan G, Zalutsky MR. Site-specific radioiodination of an anti-HER2 single domain antibody fragment with a residualizing prosthetic agent. *Nucl Med Biol.* 2021;92:171-183.

37. Mease RC, Kang CM, Kumar V, et al. An improved ^{211}At-labeled agent for PSMA-targeted α-therapy. *J Nucl Med.* 2022;63:259-267.

TABLE 1

Estimated absorbed doses for *iso*-^{211}At-SAGMB-VHH_1028 in athymic mice with subcutaneous BT474 xenografts

Tissue	Absorbed Dose (Sv/1.0 MBq)	Absorbed Dose (Sv/3.0 MBq)
Liver	3.8	11.3
Spleen	4.8	14.3
Lungs	3.7	11.2
Heart	1.8	5.4
Kidneys	14.6	43.7
Stomach	9.9	29,7
Thyroid	3.5	10.6
Sm. Int.	2.0	6.1
Lg. Int.	3.5	10.4
Muscle	0.5	1.4
Blood	1.1	3.2
Bone	0.8	2.4
Brain	0.2	0.5
Tumor	14.4	43.3

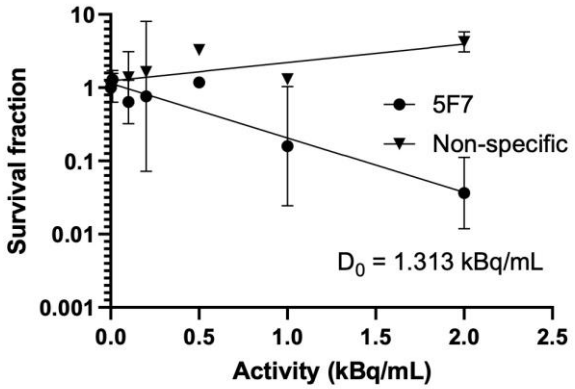

Figure 1**.** Survival fraction of BT474 breast carcinoma cells after incubation with *iso*-^{211}At-SAGMB-5F7 and HER2-irrelevant *iso*-^{211}At-SAGMB-VHH_2001.

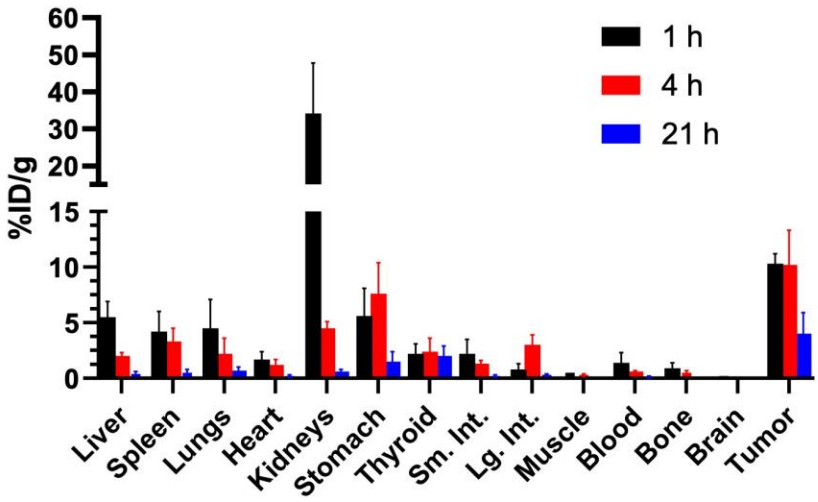

Figure 2**.** Biodistribution of *iso*-^{211}At-SAGMB-VHH_1028 in athymic mice with subcutaneous BT474 xenografts.

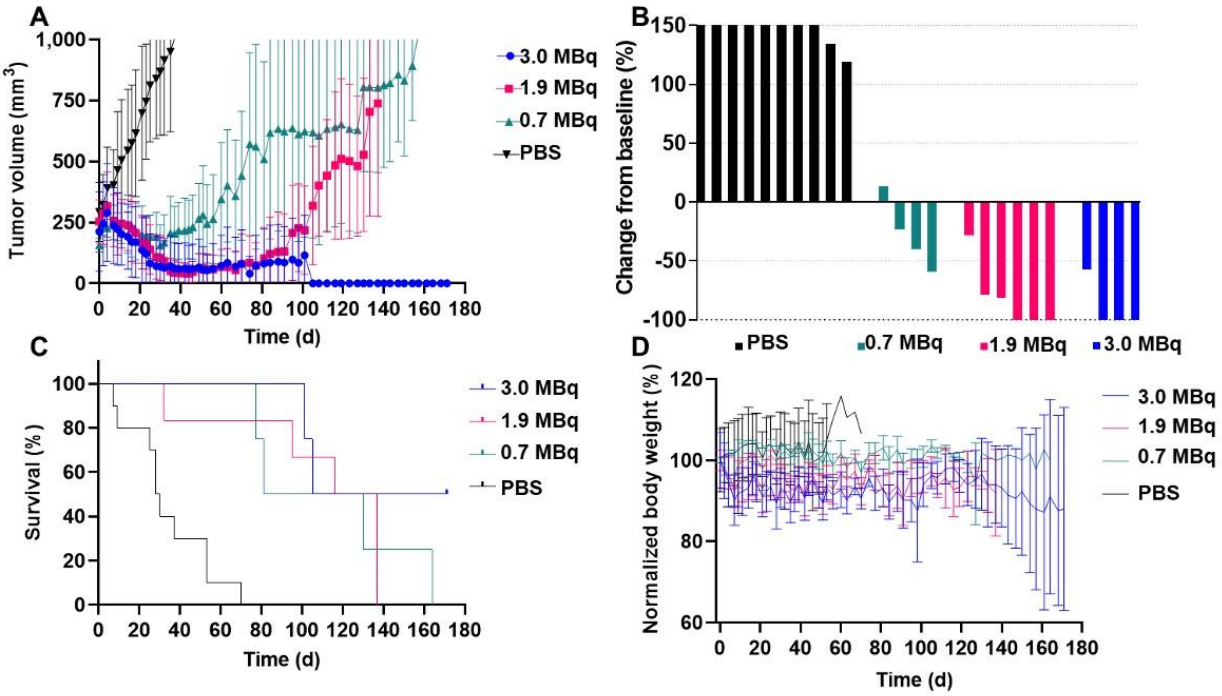

Figure 3**.** Therapeutic efficacy of single-dose *iso*-^{211}At-SAGMB-5F7 in NSG mice with BT474 xenografts. (A) tumor volume, (B) maximum tumor response waterfall plot, (C) Kaplan-Meier curve, (D) normalized body weight.

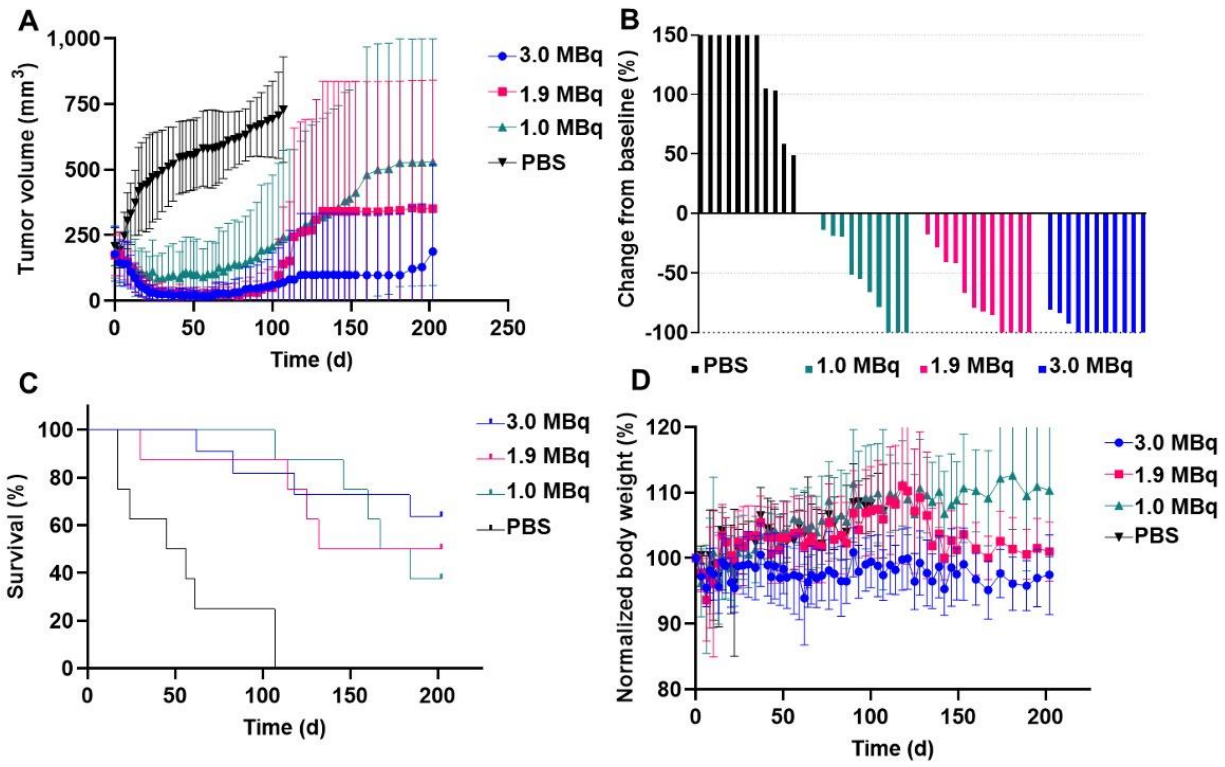

Figure 4. Therapeutic efficacy of single-dose *iso*-^{211}At-SAGMB-VHH_1028 in athymic mice with BT474 xenografts. (A) tumor volume, (B) maximum tumor response waterfall plot, (C) Kaplan-Meier curve, (D) normalized body weight.

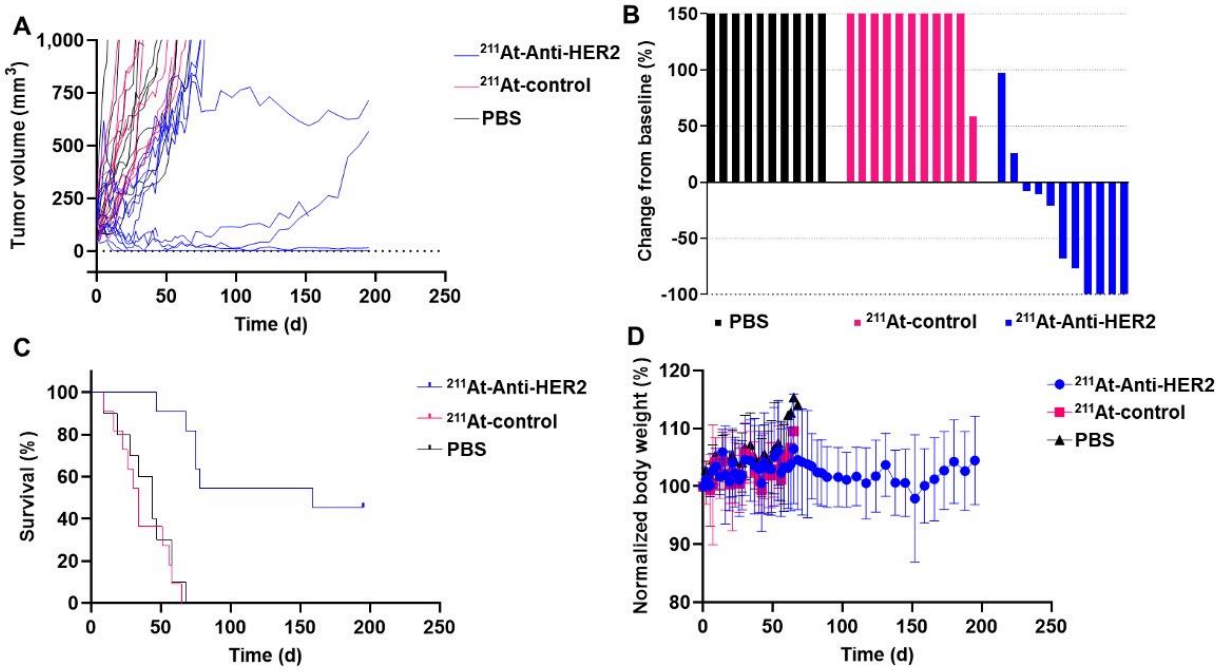

Figure 5. Therapeutic efficacy of single-dose *iso*-^{211}At-SAGMB-VHH_1028 and HER2-irrelevant *iso*-^{211}At-SAGMB-VHH_2001 in athymic mice with BT474 xenografts. (A) tumor volume in individual mice, (B) maximum tumor response waterfall plot, (C) Kaplan-Meier curve, (D) normalized body weight.

Graphical Abstract

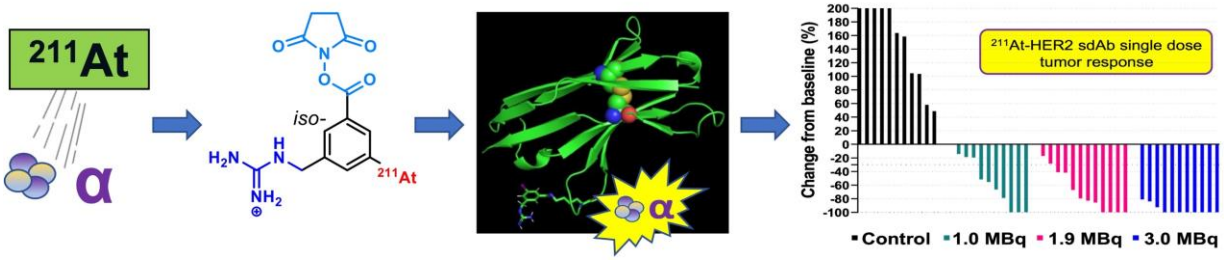

SUPPLEMENTAL METHODS

Source of Materials and General Procedures

All reagents were purchased from Sigma-Aldrich except where noted. Astatine-211 was produced on the Duke University CS-30 cyclotron by bombarding natural bismuth targets with 28 MeV α-particles via the $^{209}Bi(\alpha,2n)^{211}At$ nuclear reaction (*20*). Astatine-211 was isolated by dry distillation and trapped in PTFE tubing immersed in a cold trap, and eluted with a solution of *N*-chlorosuccinimide (NCS) in methanol (0.2 mg/mL) as previously described (*22*). *N*-succinimidyl 5-((1, 2-bis(*tert*-butoxycarbonyl)guanidino)methyl)-3-iodobenzoate (Boc_2-*iso*-SGMIB) and its corresponding tin precursor (Boc_2-*iso*-SGMTB) were synthesized as reported before (*21*). High-performance liquid chromatography (HPLC) was performed using an Agilent 1260 Infinity II System and a ScanRam RadioTLC scanner/HPLC detector combination (LabLogic; Brandon, FL). HPLC data were acquired and processed using Laura software (LabLogic). Normal-phase HPLC was performed using a 4.6 x 250 mm RX-SIL column (5 µm; Agilent, Santa Clara, CA), eluted in isocratic mode with a mixture of 0.2% acetic acid in 70:30 hexanes:ethyl acetate (v/v) at a flow rate of 1.5 mL/min. Disposable PD 10 desalting columns for gel filtration were purchased from GE Healthcare (Piscataway, NJ). Radioactivity levels in various samples were assessed using either an LKB 1282 (Wallac, Finland) or a Perkin Elmer Wizard II (Shelton, CT) automated gamma counter. Supplies for SDS PAGE were obtained from Invitrogen/ThermoFisher Scientific (Waltham, MA).

Quality Control of *iso*-^{211}At-SAGMB-sdAb Conjugates

The radiochemical purity (RCP) of the three *iso*-^{211}At-SAGMB-sdAb conjugates was determined by SDS PAGE, which was performed using NuPage 10% Bis-Tris gels and

NuPage MES SDS running buffer (20X) in an Invitrogen mini gel tank. Labeled sdAbs in 25 µL PBS were mixed with 25 µL of NuPage LDS sample buffer (4X). After loading 20 µL (~11 kBq) of ^{211}At-labeled sdAbs in duplicate lanes along with protein standards (PageRuler™ Plus Prestained Protein Ladder, 10 to 250 kDa), electrophoresis was performed at 250 V for 15-20 min. The gels were exposed to a phosphor plate for 1 min before imaging with Cyclone Plus scanner. In some cases, gel-permeation HPLC (GPC) also was used to determine RCP. For this, an Agilent PL Multisolvent 20 column (7.8 x 150 mm) was eluted in isocratic mode with pure Milli-Q® water as the mobile phase at a flow rate of 0.3 mL/min. Under these conditions, the sdAbs elute with a retention time of 3 min.

Cells and Cell Culture Conditions

Cell culture reagents were purchased from Invitrogen (Grand Island, NY). The BT-474 human breast carcinoma cell line (ATCC No. HTB-20) was cultured in Dulbecco's Modified Eagle's Medium (DMEM) containing 10% FBS and supplemented with 10 mg/mL bovine insulin. Cells were cultured at 37^{o}C in a 5% CO_2 atmosphere.

Cell Survival Assay

BT474 cells were seeded into six well plates at a concentration of 2.5 x 10^5 cells per well before incubating overnight under appropriate cell culture conditions to allow the cells to adhere to the plate. On the day of the experiment, media was aspirated from the wells before replacing with media containing increasing concentrations, in triplicate, of *iso*--^{211}At-SAGMB-5F7. A preliminary dose finding experiment was performed with activity concentrations from 0 to 1000 kBq/mL, and then a dose range of 0 to 2.0 kBq/mL was selected for further evaluation. After a 2-h incubation, each well was aspirated and

washed three times with 1 mL PBS. Cells from each well were detached by incubation with 0.5 mL of trypsin at 37°C for 3 min before collection with 1 mL of fresh medium. Cells were transferred to sterile tubes, counted and then reseeded into T25 flasks and incubated at 37°C for 14 days at which point cells were again detached with trypsin and counted. The cytotoxicity of *iso*-^{211}At-SAGMB-VHH_2001, which served as a HER2-unreactive control, was measured in parallel in identical fashion. Survival fractions were plotted as a function of initial activity concentration. The D_0 (dose to reduce survival to 37% on the exponential portion of the curve) and 95% confidence limits of the regression fit were determined using linear regression on GraphPad Prism 9 following a reported method (*28*).

Statistics

Data are presented as mean ± standard deviation. Statistical and data analysis for the therapeutic efficacy studies was performed as follows: for each group, the average body weight and the standard deviation were calculated and plotted versus time. Normalized average body weight was calculated by setting the initial average body weight on the day of treatment (Day 0) to 100%. Animals were excluded at the day of death. Two-tailed paired t tests were conducted for the normalized average body weight between each group, and tests were only conducted for days when alive animals were present in each group. Average tumor volumes and standard deviations were calculated for each group and plotted versus time. When animals died or were euthanized, their tumor volume at the day of death was carried forward after the day of death for the calculation of average tumor volume. Two-tailed paired t tests were conducted for the average tumor

volumes between each group, and tests were only conducted for days when animals remained alive in each group. Differences with a *P* value < 0.05 were considered statistically significant. For survival data, log-rank (Mantel-Cox) test, log-rank test for trend, and Gehan-Breslow-Wilcoxon test were conducted. Maximum tumor response waterfall plots were generated for the therapy studies by recording the maximum tumor response (growth or inhibition) for each mouse during the experimental period. Tumor growth inhibition (TGI) was calculated as follows:

$$TGI = \left(1 - \frac{Normalized\ Average\ Tumor\ Volume\ of\ Treatment\ Group\ on\ Day\ X}{Normalized\ Average\ Tumor\ Volume\ of\ Control\ Group\ on\ Day\ X}\right) \times 100\%$$

TGI was plotted as a function of time. All data analyses were performed using GraphPad Prism 9.

Supplemental Tables

Supplemental Table 1. Experimental details for the single-dose *iso*-^{211}At-SAGMB-5F7 therapy study in NOD SCID mice bearing subcutaneous BT474 breast carcinoma. xenografts.

Group	Initial Tumor Volume (mm^3)	^{211}At Dose (MBq)	sdAb Dose (μg)
PBS control	293.2 ± 120.5	0	0
Low dose	157.1 ± 27.7	0.7	3
Medium dose	253.8 ± 88.3	1.9	8.5
High dose	212.5 ± 163.6	3.0	14

Supplemental Table 2. Experimental details for the single-dose *iso*-^{211}At-SAGMB-VHH_1028 therapy study in athymic mice bearing subcutaneous BT474 breast carcinoma. xenografts.

Group	Initial Tumor Volume (mm^3)	^{211}At Dose (MBq)	sdAb Dose (μg)
PBS control	207.7 ± 73.3	0	0
Low dose	186.9 ± 99.9	1.0	10.6
Medium dose	174.4 ± 77.4	1.9	17.8
High dose	178.3 ± 102.4	3.0	16.7

Supplemental Table 3. Experimental details for the comparison of the therapeutic effectiveness of *iso*-^{211}At-SAGMB-VHH_1028 and *iso*-^{211}At-SAGMB-VHH_2001 nonspecific sdAb in athymic mice bearing subcutaneous BT474 breast carcinoma xenografts.

Group	Initial Tumor Volume (mm^3)	^{211}At Dose (MBq)	sdAb Dose (μg)
PBS control	126.8 ± 80.3	0	0
iso-^{211}At-SAGMB-VHH_1028	120.7 ± 49.5	1.0	3
iso-^{211}At-SAGMB-VHH_2001	120.6 ± 69.7	1.1	3.7

Supplemental Table 4. Biodistribution of *iso*-^{211}At-SAGMB-VHH_1028 anti-HER2 sdAb in athymic mice bearing subcutaneous BT474 breast carcinoma xenografts.

Percent injected dose per gram of tissue[a]			
Tissues	1 h	4 h	21 h
Liver	5.48 ± 1.42	1.96 ± 0.25	0.43 ± 0.19
Spleen	4.24 ± 1.82	3.31 ± 1.23	0.51 ± 0.29
Lungs	4.50 ± 2.61	2.15 ± 1.38	0.72 ± 0.31
Heart	1.67 ± 0.72	1.15 ± 0.50	0.24 ± 0.12
Kidneys	34.20 ± 13.63	4.46 ± 0.62	0.57 ± 0.23
Stomach	5.61 ± 2.51	7.61 ± 2.77	1.49 ± 0.87
Thyroid[b]	0.42 ± 0.18	0.53 ± 0.25	0.38 ± 0.17
Sm. Int.	2.24 ± 1.29	1.28 ± 0.28	0.24 ± 0.08
Lg. Int.	0.77 ± 0.54	2.98 ± 0.93	0.33 ± 0.12
Muscle	0.53 ± 0.04	0.27 ± 0.07	0.09 ± 0.04
Blood	1.41 ± 0.89	0.58 ± 0.13	0.14 ± 0.05
Bone	0.92 ± 0.53	0.52 ± 0.21	0.13 ± 0.05
Brain	0.15 ± 0.04	0.10 ± 0.03	0.03 ± 0.01
Tumor	10.28 ± 0.90	10.21 ± 3.10	4.00 ± 1.90

[a]Mean ± SD (n=5); [b]% injected dose/organ

Supplemental Table 5. Biodistribution of *iso*-^{211}At-SAGMB-VHH_2001 anti-GFP sdAb in athymic mice bearing subcutaneous BT474 breast carcinoma xenografts.

Percent injected dose per gram of tissue[a]			
Tissues	1 h	4 h	21 h
Liver	7.29 ± 0.95	2.60 ± 0.49	0.31 ± 0.09
Spleen	7.57 ± 2.01	4.63 ± 1.06	1.03 ± 0.64
Lungs	4.97 ± 1.57	3.85 ± 0.36	1.00 ± 0.45
Heart	2.12 ± 0.20	1.39 ± 0.27	0.35 ± 0.20
Kidneys	68.18 ± 11.15	5.46 ± 0.94	0.65 ± 0.22
Stomach	16.36 ± 3.66	18.56 ± 3.67	3.01 ± 1.84
Thyroid[b]	0.62 ± 0.21	1.02 ± 0.21	1.13 ± 0.86
Sm. Int.	1.96 ± 0.28	1.84 ± 0.32	0.40 ± 0.26
Lg. Int.	0.86 ± 0.06	2.38 ± 0.42	0.32 ± 0.16
Muscle	0.94 ± 0.10	0.53 ± 0.21	0.12 ± 0.06
Blood	1.55 ± 0.35	0.73 ± 0.07	0.19 ± 0.09
Bone	1.25 ± 0.08	0.82 ± 0.15	0.18 ± 0.05
Brain	0.20 ± 0.02	0.13 ± 0.01	0.04 ± 0.02
Tumor	3.17 ± 0.50	2.05 ± 0.23	0.58 ± 0.31

[a]Mean ± SD (n=5); [b]% injected dose/organ

Supplemental Table 6. Paired-label biodistribution of *iso*-^{125}I-SGMIB-5F7 and *iso*-^{131}I-SGMIB-VHH_1028 in athymic mice bearing HER2-expressing SKOV-3 ovarian carcinoma xenografts.

	Percent injected dose per gram[a]					
	1 h		4 h		24 h	
tissue	5F7	VHH_1028	5F7	VHH_1028	5F7	VHH_1028
Liver	5.86 ± 0.73	5.15 ± 0.45	2.11 ± 0.49	1.88 ± 0.45	0.43 ± 0.04	0.31 ± 0.03[c]
Spleen	1.96 ± 0.57	1.62 ± 0.44	0.64 ± 0.23	0.52 ± 0.18	0.15 ± 0.04	0.13 ± 0.02
Lungs	1.76 ± 0.16	2.72 ± 0.41[c]	0.31 ± 0.12	0.57 ± 0.15[c]	0.06 ± 0.03	0.06 ± 0.02
Heart	0.55 ± 0.06	0.67 ± 0.08	0.13 ± 0.02	0.17 ± 0.02	0.02 ± 0.01	0.03 ± 0.02
Kidneys	43.56 ± 8.26	42.63 ± 7.79	2.72 ± 0.60	2.80 ± 0.61	0.12 ± 0.07	0.12 ± 0.06
Stomach	1.30 ± 0.43	0.95 ± 0.34	0.65 ± 0.09	0.44 ± 0.06[c]	0.02 ± 0.01	0.02 ± 0.01
Sm. Int.	1.33 ± 0.34	1.32 ± 0.41	0.52 ± 0.15	0.51 ± 0.17	0.02 ± 0.01	0.02 ± 0.01
Lg. Int.	0.27 ± 0.22	0.25 ± 0.19	1.71 ± 0.71	1.76 ± 0.61	0.08 ± 0.07	0.07 ± 0.06
Muscle	0.24 ± 0.15	0.22 ± 0.10	0.05 ± 0.02	0.03 ± 0.01	0.01 ± 0.01	0.01 ± 0.00
Blood	0.92 ± 0.38	1.05 ± 0.24	0.16 ± 0.01	0.26 ± 0.05[c]	0.06 ± 0.05	0.04 ± 0.01
Brain	0.09 ± 0.08	0.09 ± 0.07	0.01 ± 0.00	0.01 ± 0.01	0.02 ± 0.01	0.01 ± 0.01
Thyroid[b]	0.10 ± 0.09	0.08 ± 0.07	0.09 ± 0.02	0.04 ± 0.04	0.09 ± 0.04	0.04 ± 0.02
Tumor	7.52 ± 4.90	7.46 ± 4.60	9.34 ± 3.95	9.30 ± 4.00	3.83 ± 2.05	3.52 ± 2.13

[a]mean ± SD, n=5; [b]Percent injected dose in thyroid; [c]Difference statistically signficant P <0.05

Supplemental Figures

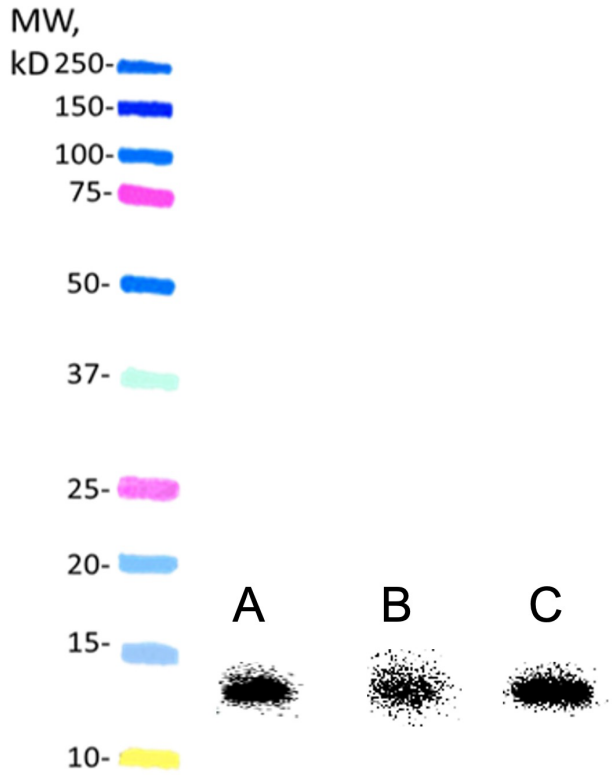

Supplemental Figure 1. SDS-PAGE phosphor imaging of ^{211}At-labeled sdAbs. A: *iso*-^{211}At-SAGMB-5F7; B: *iso*-^{211}At-SAGMB-VHH_1028; C: *iso*-^{211}At-SAGMB-VHH_2001.

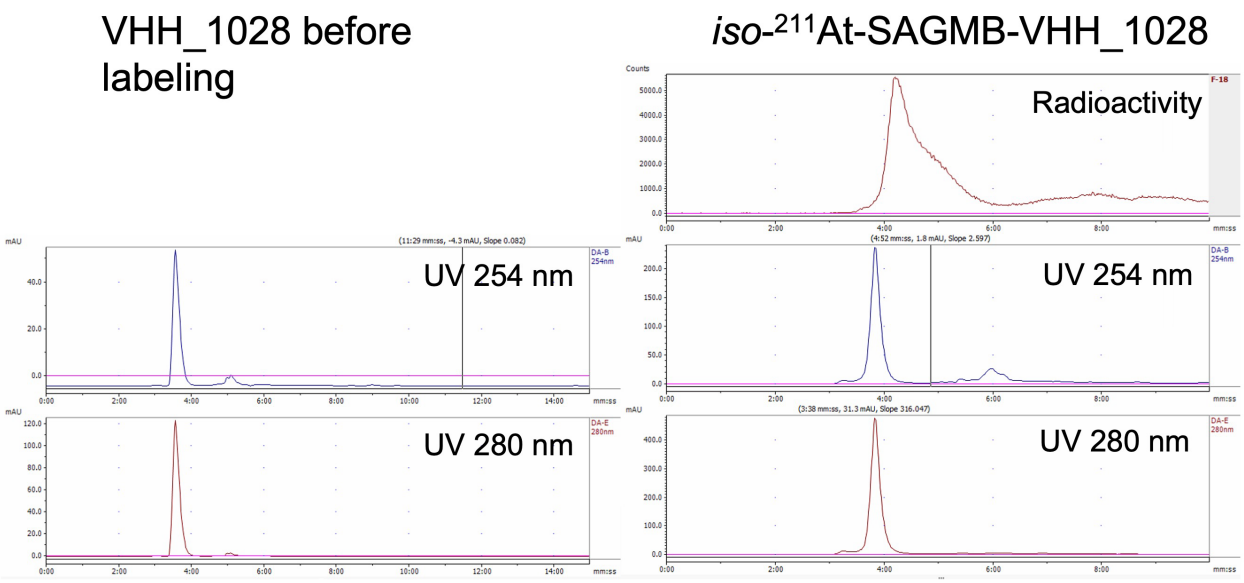

Supplemental Figure 2. Representative gel permeation chromatography (GPC-HPLC) profiles obtained on Agilent GPC column eluted at a flow rate of 0.3 mL/min with water containing 0.1% formic acid. Left; VHH_1028 HER2-specific sdAb before labeling. Right; *iso*-^{211}At-SAGMB-VHH_1028.

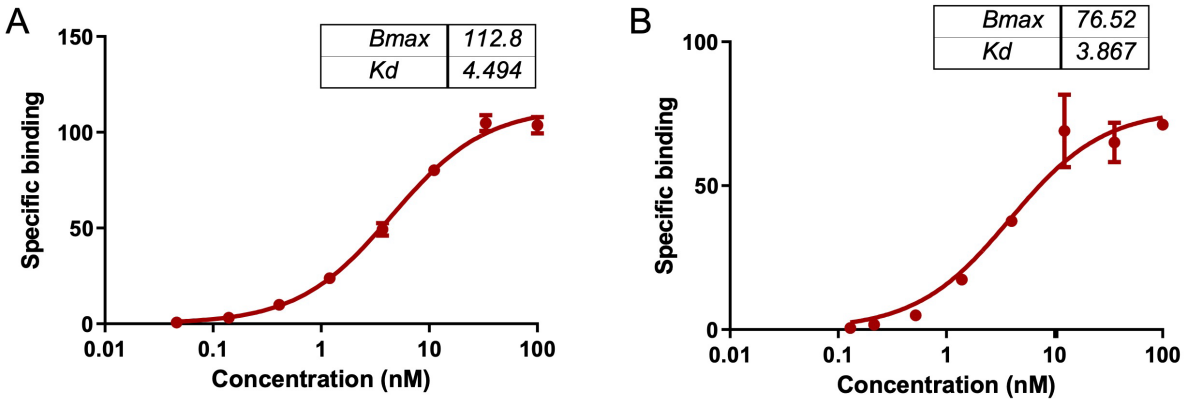

Supplemental Figure 3. Saturation binding assays performed on HER2-positive BT474 breast carcinoma cells with (A) *iso*-^{211}At-SAGMB-5F7 and (B) *iso*-^{211}At-SAGMB-VHH_1028. Nonspecific binding was determined by co-incubation with a 100-fold excess of trastuzumab as described in the text.

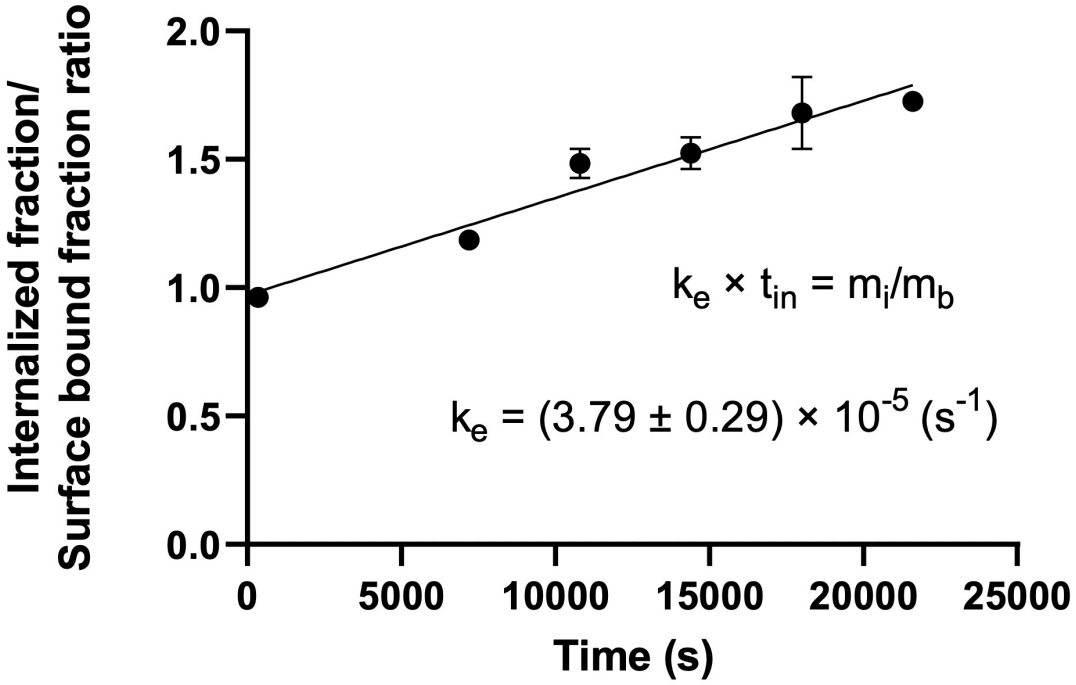

Supplemental Figure 4. Ratio of internalized-to-cell surface bound ^{211}At activity as a function time after incubation *iso*-^{211}At-SAGMB-5F7 with BT474 breast carcinoma cells. The internalization rate constant, k_e, was calculated by linear regression analysis as described in the text.

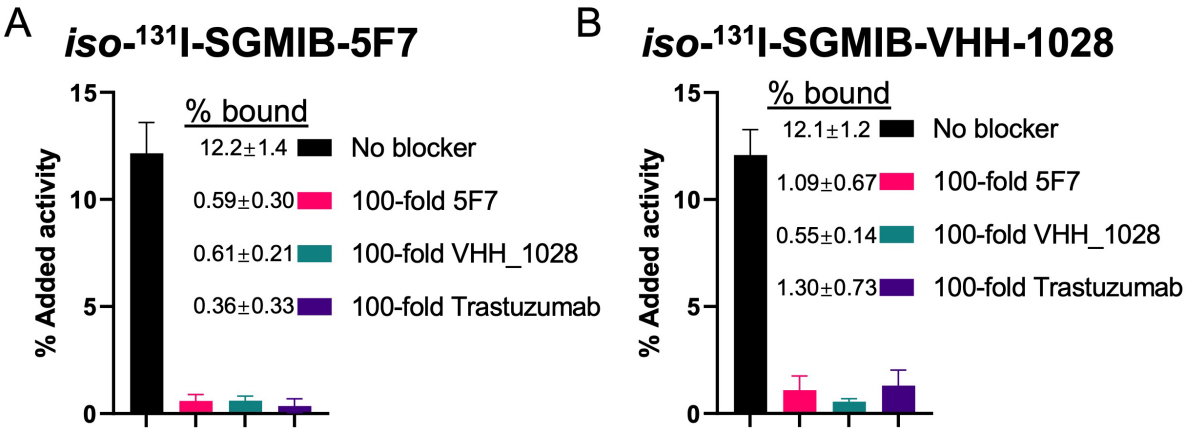

Supplemental Figure 5. Binding of (A) *iso*-^{131}I-SGMIB-5F7 and (B) *iso*-^{131}I-SGMIB-VHH_1028, labeled as described [21], to HER2-expressing BT474 breast carcinoma cells. Approximately 8 × 10^4 BT474 cells per well were plated on a 24-well plate overnight. The radioiodinated VHH conjugates (37 kBq, 0.13 µg) were added and incubated at 37°C for 1 h in triplicate with/without a 100-fold molar excess of 5F7, VHH_1028 or trastuzumab. Cell-associated activity calculated as percentage of added activity bound to the cells.